

## Experimental Investigation on Performance Characteristics of a Small-Scale Rotating Detonation Engine

Mohd Fahmi Md Salleh<sup>1,2\*</sup>, Mazlan Abdul Wahid<sup>1</sup>, Ab Aziz Mohd Yusof<sup>2</sup>, Umar Ikhwan Mohd Rozaiddin<sup>3</sup>, Natrah Kamaruzaman<sup>1</sup>, Hazim Sharudin<sup>2</sup>, Haszeme Abu Kasim<sup>2</sup>

<sup>1</sup>*High Speed Reacting Flow Laboratory (HiREF), Faculty of Mechanical Engineering, Universiti Teknologi Malaysia,  
81310 Skudai, Johor, Malaysia*

<sup>2</sup>*Faculty of Mechanical Engineering, Universiti Teknologi MARA, Johor Branch, Pasir Gudang Campus,  
81750 Masai, Johor, Malaysia*

<sup>3</sup>*West Virginia University, Morgantown, West Virginia 26506-6106 United States of America*

---

### ARTICLE INFO

*Article history:*

Received 30 April 2025

Revised 13 July 2025

Accepted 26 September 2025

Online first

Published 15 January 2026

*Keywords:*

Rotating detonation

Detonation combustor

Small-scale

Stability

Methane

*DOI:*

10.24191/jmeche.v23i1.6123

---

### ABSTRACT

A small-scale rotating detonation engine (RDE) is a detonation-based engine with potential propulsion and power generation applications, especially when weight and space are critical factors. In this study, experimental investigations on a small-scale RDE were fueled with a low methane-oxygen mixture flow rate to investigate the performance characteristics, including the detonation wave stability, detonation wave velocity, and thrust generated. The inner and outer annulus diameters of the small-scale RDE are 38 mm and 46 mm, respectively. The total mass flow rate,  $\dot{m}_{total}$ , of the methane-oxygen mixture employed in the present study was 0.0040 kg/s, and the equivalence ratios,  $\varphi$ , range from 0.8 to 1.2. The result shows two types of instability observed within the tested equivalence range: chaotic instability and waxing and waning instability. The least instability was observed at  $\varphi = 1.0$ , which can be considered the optimal mixture proportion for a stable, small-scale RDE operation. The average detonation wave velocity and thrust were found to increase as the equivalence ratio increased. Meanwhile, the average detonation pressure within the RDE annulus was observed to rise, reaching a maximum value, and decreasing as the equivalence ratio increases. Thus, achieving a well-balanced reactant mixture is important to ensure a stable detonation wave propagation and optimize the overall RDE performance.

---

<sup>1\*</sup> Corresponding author. *E-mail address:* fahmisalleh@uitm.edu.my  
<https://doi.org/10.24191/jmeche.v23i1.6123>

## INTRODUCTION

Most of the existing combustors operate in deflagration combustion mode as the standard mode of operation. Current issues, such as emissions, energy output, and fuel consumption rates, require continuous research to improve the efficiency of the combustion systems. One of the approaches to further enhance the combustion system is the implementation of detonation combustion mode, which has the potential to offer more advantages than deflagration combustion mode. Generally, the detonation combustion mode is characterised by a supersonic combustion wave tightly coupled with the exothermic reaction zone (Rui et al., 2016). This situation causes the pressure and temperature to increase abruptly while slightly decreasing the specific volume as the shock front passes through the reactant mixture (Driscoll, 2016).

As a result, the detonation combustion mode has a smaller entropy increment with faster heat release, which leads to higher thermal efficiency (Rui et al., 2016). Furthermore, detonation combustion mode generates higher temperature, pressure, and density with higher combustion speed, concerning the same amount of fuel as compared to the deflagration combustion mode (Rahman, 2021). Additionally, a shorter chemical reaction initiation time can be obtained since the detonation combustion wave travels at supersonic speed (Raman et al., 2023). A previous report on the theoretical efficiency of detonation-based thermodynamic cycle has found that detonation combustion mode may improve the Brayton cycle by approximately 20-50% (Heiser & Pratt, 2002).

These factors have become the motivation for the investigations into detonation-based devices for approximately six decades. One of the detonation-based devices that received significant research interest from previous researchers is the rotating detonation engine (RDE). The application of RDE can be considered promising in enhancing future propulsion technologies and the power generation cycle. This is due to the construction and the operation of the RDE, which was reported to be simpler and cost-effective compared to the other detonation-based devices, especially the pulse detonation engine (PDE) (Rui et al., 2016). This can be evidenced by the RDE operational characteristics, which require only a single initiation to continuously propagate the detonation waves within the combustion chamber and generate near-uniform thrust (Liu et al., 2023).

Unlike RDE, PDE allocates 45% of the operating cycle to non-productive activities such as fuel loading and scavenging before generating detonation. This scenario reduces the performance of the PDE due to large pressure oscillations (Hoke et al., 2005) and limited detonation frequency (Zhu et al., 2020) produced during the operation. Furthermore, RDE detonation propagation frequency is higher than PDE, which can be 1 kHz – 100 kHz (Liu et al., 2023). Higher operating frequency of the RDE may result in continuous operating engines with higher propulsive performance and stability. However, the detonation frequency of the RDE is highly influenced by the fuel composition, equivalence ratio, and geometry (Barnouin et al., 2025; Rankin et al., 2015).

Fig 1 illustrates a conceptual overview of an RDE operation. Generally, the RDE has an annular combustion chamber formed by the arrangement of two coaxial cylinders (Hu & Zhang, 2024). Meanwhile, the fuel and oxidizer supplied to the RDE combustion chamber flows through the designated ports to a number of micro-nozzles or slits placed before the inlet of the annulus. The reactant mixture was then initiated using either direct ignition or the gradient ignition method (Goodwin et al., 2016). One of the standard initiation methods is the gradient ignition, which can occur inside or before the RDE combustion chamber. This approach uses a specific type of initiator tube known as a pre-detonator to facilitate the deflagration-to-detonation transition (DDT) process before the RDE combustion chamber. The usage of the pre-detonator provides a high success rate and repeatability in RDE initiations (Kindracki et al., 2011). Once the combustion wave enters the RDE combustion chamber tangentially, one or multiple continuous rotating detonation waves are formed and continuously propagate within the annulus circumference (Rui et al., 2016). The high-pressure and high-temperature combustion products established behind the shock wave

and flow out to the RDE open coaxial end downstream to produce thrust (Rui et al., 2016). This process will continue to perform as long as the reactant mixture is supplied to the RDE combustion chamber.

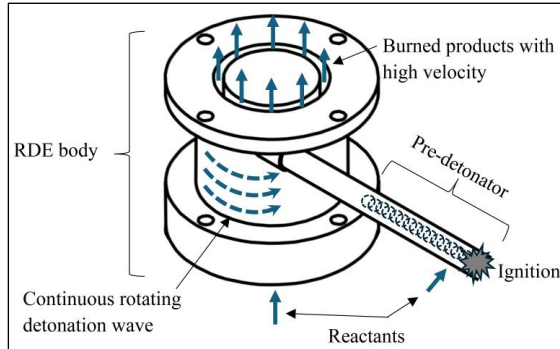


Fig. 1. General operation of RDE.

Previous researchers have extensively examined several key areas to gain a comprehensive understanding of the RDE operational behavior (Rahman, 2021). The key areas include detonation wave structure, detonation wave velocity, thrust generation, and detonation wave stability. Most previous studies commonly employed several key areas simultaneously in parametric studies investigating the influence of various factors, including the type of reactant, equivalence ratio, mass flow rate, and the geometrical configurations of the RDE. Note that the key areas listed previously are well known to be interdependent and are important in characterizing the performance of the RDE operation. For example, the stability of the detonation wave is important to ensure that the RDE can continuously produce consistent thrust. Furthermore, the detonation wave velocity represents the propagation speed of the detonation wave within the annulus, which influences the thrust output during the RDE operation.

One of the important RDE key areas frequently investigated by previous researchers is detonation wave stability during RDE operations. This is because the detonation wave stability directly influences the detonation wave velocity, affecting the magnitude and consistency of the thrust generated during the RDE operation. Anand et al. (2016) reported four instabilities observed in the RDE operation: chaotic instability, waxing and waning instability, mode switching instability, and longitudinal pulsed detonation (LPD) instability. Each of these instabilities show different characteristics as reflected in the pressure profiles, which are influenced by specific and various factors.

The first instability is chaotic instability, which can be observed by the extremely incoherent and chaotic pressure profiles of the detonation wave propagation. According to Anand et al. (2016), improper mixing is considered the cause of chaotic instability, as it results from the effects of pressure feedback on reactant injection. Such conditions can contribute to periodic failure and reinitiation of the detonation wave. Note that lower injection pressure ratios may occur when the air flow rates are low, and the RDE operation may experience higher pressure feedback from the detonation wave. This situation led to variations in the recovery time of the reactant's injection after the detonation propagation (Driscoll et al., 2015; Paxson et al., 2015).

Another RDE instability observed is known as waxing and waning instability (Anand et al., 2016). In waxing and waning instability, the pressure peak shows periodic waxing and waning in strength which can be seen as low frequency oscillations that are considered as a detonation wave packet that contains numerous consecutive cycles of rotating detonation (Kindracki, 2015). Occasionally, the detonation wave packet may end with wave structure breakdown and a period of unstable pressure comparable to chaotic instability. The scenario of waxing and waning may be due to the detonation wave blocking and unblocking

the fuel injectors in a cyclic loop. This situation resulted in significant RDE air supply fluctuation that caused periodic changes to the detonation wave intensity, leading to waxing and waning instability during the RDE operation.

Instantaneous change between the operating modes is defined by the number of detonation waves in the RDE annulus, referred to as mode switching instability. Lin et al. (2015) have reported that the pressure is almost half of the one detonation wave mode for the two-detonation wave mode in the RDE combustion chamber. Multiple detonation waves may be advantageous due to lower individual waves' pressure, which reduces the effect towards the fuel and oxidizer supply disruption and leads to high stability compared to the lower wave modes. Although multiple detonation wave modes may be preferred in RDE operation due to their stable and less reactants supply disruption characteristics, the abrupt switching between them contributed to a strong RDE operation instability.

Lastly, Anand et al. (2016) have further described longitudinal pulsed detonation (LPD) instability. LPD is pulsed, and high-amplitude pressure fluctuations occur azimuthally and simultaneously with the same rotating detonation wave magnitude at high frequency. However, the described phenomenon is considered as axial pressure oscillations rather than azimuthal inside the RDE combustion chamber by Bykovskii et al. (2006) and Bykovskii & Vedernikov (2003). LPD can be characterized by axially moving waves travelling above sonic speed, driven by pulsations, and is classified as a detonation event. To identify the LPD instability, several sensors must be distributed azimuthally at the RDE combustion chamber. (Anand et al., 2015)

Previously, various RDE geometries have been studied, including the conventional circular annular, hollow, and asymmetric. In recent years, investigations into the small-scale RDE have captured the attention of the researchers (Armbruster et al., 2024). This is due to the compact option offered by small-scale RDE which benefits the power generation and application where the space and weight is critical especially in thrust generation (Dechert et al., 2020). Moreover, the small-scale RDE is well suited for laboratories studies where the testing environment is limited and can be scaling up to a larger design in the future (Armbruster et al., 2024). Furthermore, operating the RDE at lower mass flow rates contributes to enabling the potential of the RDE for further size reduction. However, different RDE combustor sizes and operating conditions, such as the lower total mass flow rate, may vary the RDE operation characteristics. This is because the performance of the RDE is affected by various factors, including the chemical processes, specific geometric parameters, and flow conditions that contribute towards the complexity of a successful RDE operation despite the simple operation (Dechert et al., 2020).

One of the reasons is a shorter distance travelled by the detonation wave to reach the same point. This imposes challenges for the reactant mixture refresh rates and mixing time during the RDE operation (Law et al., 2021). Insufficient mixing can lead to premature deflagration, weaker detonation waves, and slower heat release, all of which fail to sustain the detonation wave (Prakash et al., 2021). Additionally, small detonation channel radius may result in detonation instability established within the RDE combustion chamber (Kudo et al., 2011). Thus, this study aims to gain a depth understanding of the performance characteristics of a small-scale RDE fueled by a low methane-oxygen mixture flow rate. The experimental work involves with a range of equivalence ratios, which can be considered as an independent parameter of the reactant mixture, with a constant total mass flow rate to examine the performance characteristics of a small-scale RDE, including the detonation stability, detonation wave velocity, and thrust generated during the operation.

## METHODOLOGY

This study conducted the experimental work at High Speed Reacting Flow Laboratory (HiREF), Universiti Teknologi Malaysia (UTM). The RDE experimental rig was set up in the test chamber equipped with a ventilation system to exhaust the combustion products and excess fuel gases. Furthermore, the operation of the RDE has been controlled from a control room, allowing for remote operation, control, and data collection. The following sections will discuss the RDE test model, RDE control system, and the measuring devices used in this study.

### RDE test model

A common annular RDE design that the previous researchers studied was used in this study. The design was selected due to its simplicity and effectiveness in sustaining detonation wave propagation (Bykovskii et al., 2018; Frolov et al., 2015). Furthermore, the geometrical parameters for the RDE test model in this study have been determined based on the recommendations provided by Bykovskii et al. (2006), Dechert et al. (2020) and Han et al. (2021). From the analysis, the reactant mixture fill height was estimated to be approximately 20.3 mm from the fuel-oxidizer injection surface. Meanwhile, the detonation channel length chosen for the current RDE design is 50 mm, slightly longer than the minimum detonation channel length estimated to ease the fabrication process. Moreover, the annulus outer diameter selected for this study is 46 mm, within the calculated annulus outer diameter range with a 4 mm detonation channel gap.

The current RDE test model implements the modular concept to ease the fabrication, installation, and future modification. Generally, there are seven separate modules for the RDE test model construction as presented by Table 1 and Fig 2. These include a base plate, an oxidizer ring, a mixing ring, a fuel injection body, a centre body, an outer body, and a pre-detoner. The RDE test model was fabricated using mild steel due to lower fabrication cost. The assembly of the RDE test model has a total length,  $L_{total}$ , of 100 mm with RDE combustor length,  $L_{combustor}$ , of 50 mm. In the present study, no nozzle has been attached to the RDE test model, such as the aerospike nozzle, to get a clear detonation chamber annulus visualisation during experiments similar to a study conducted by Armbruster et al. (2024).

On the other hand, the reactant mixing method used in this study was designed according to a study conducted by Rahman et al. (2020) which is the radially outward fuel injection and axial oxidizer injection. It was said that effective mixing between the fuel and oxidizer in axial and radial manners could potentially be achieved. This is due to the direct collision between the fuel stream and the oxidizer stream entering the chamber, resulting in lower maximum mass fraction values. Furthermore, the fuel was supplied from the base of the RDE and entered the RDE mixing area through 80 injection holes with 0.7 mm diameter (Dairobi G et al., 2021). Meanwhile, the oxidizer is supplied to the RDE through four tangential injection ports at the oxidizer ring before flowing in an axial direction through the channel and mixing with the injected fuel at the mixing point before the reactant mixture enters the RDE annulus.

Table 1. General dimensions for the RDE test model

Item	Dimension
Combustor length, $L_{combustor}$	50 mm
Combustor annulus:	
Inner diameter	38 mm
Outer diameter	46 mm
Mixing area	1 mm gap round slot
Fuel injection body	$\varnothing$ 0.7 mm $\times$ 80 fuel injection holes
Total RDE Length, $L_{total}$	100 mm

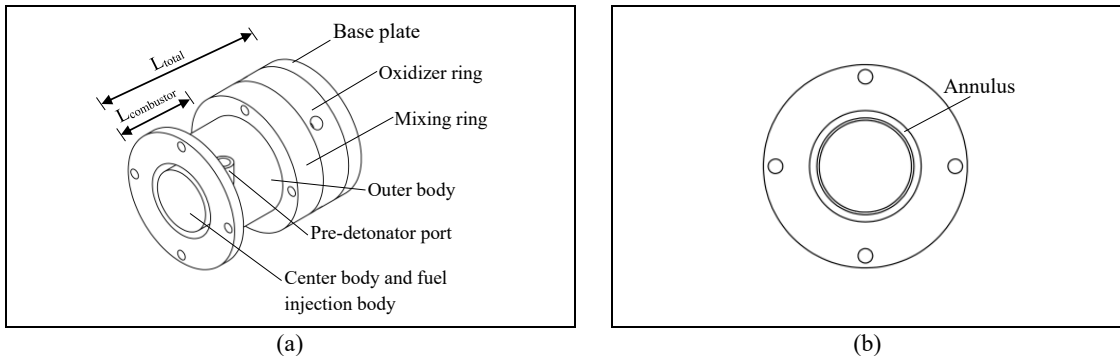


Fig. 2. Small-scale RDE (a) modular arrangement and (b) front view.

The RDE outer body design was developed to facilitate the installation of the high-frequency ICP pressure sensor. The outer body thickness for both outer body designs was set constant at 10 mm with a six mm-thick flange attached to one end of the outer body for the RDE test model assembly. The high-frequency ICP pressure sensor was positioned at an angle of 45° opposite to the pre-detonator location. Moreover, the high-frequency ICP pressure sensor was placed near the reactant fill height, 28 mm upstream of the open-end RDE exhaust.

In this study, a pre-detonator with a total length of 220 mm was tangentially positioned 13 mm upstream from the RDE open-end exhaust. This pre-detonator position was selected since the reactant mixing improves along the RDE combustion chamber and may improve the initiation and transition to steady detonation operation as suggested by Mazlan et al. (2021). Furthermore, the same detonation channel gap has been applied to the pre-detonator inner diameter, which is 4 mm. Also, a Shchelkin spiral with a length of 160 mm was placed inside the pre-detonator to increase the resistance inside and promote the DDT.

### RDE control system

The RDE control systems, as shown in Fig 3, consist of three subsystems: fuel-oxidizer feeding, ignition initiation, and sequential control. The RDE control systems have been developed to ensure the smooth and successful operation of the RDE in this study. The fuel-oxidizer feeding functions to transport the designated gases to the pre-detonator and RDE from the gas storage room. Acetylene-oxygen and methane-oxygen were chosen as the fuel-oxidizer for the pre-detonator and RDE combustion chamber in this study, respectively. The selection of acetylene-oxygen mixture for the pre-detonator is due to the high reactivity characteristics, where an optimal detonation propagation in the RDE may be reached by using this mixture, as suggested by Mazlan et al. (2023). The equivalence ratio for the acetylene and oxygen was set at 1.2, which is considered slightly fuel rich. According to Li et al. (2018), a slightly fuel-rich fuel-oxidizer mixture can improve the success rate of the supersonic combustion initiation. On the other hand, methane-oxygen mixture has been used as the reactant to power the RDE in this study due to its availability and cost-effective source of energy (Prakash et al., 2021). The equivalence ratio of 0.8 to 1.2, and total mass flow rate of 0.0040 kg/s, were used for the methane-oxygen mixture in this study.

Besides, the detonation wave was introduced to the RDE combustion chamber with the aid of the pre-detonator, which was linked to the ignition initiation subsystem. The ignition initiation subsystem is composed of a pulse ignition system connected to a spark plug positioned at the top of the pre-detonator and linked to the RDE control panel. The spark plug will produce sparks after the pulse ignition system receives a signal from the control panel and is activated. Furthermore, the sequence of the fuel-oxidizer feeding and ignition initiation during the RDE operation was controlled by sequential control. The integration of these systems facilitates future maintenance and modification, increases safety, and simplifies

the control of RDE. The activation of components related to fuel-oxidizer feeding and ignition initiation was coordinated using a microcontroller.

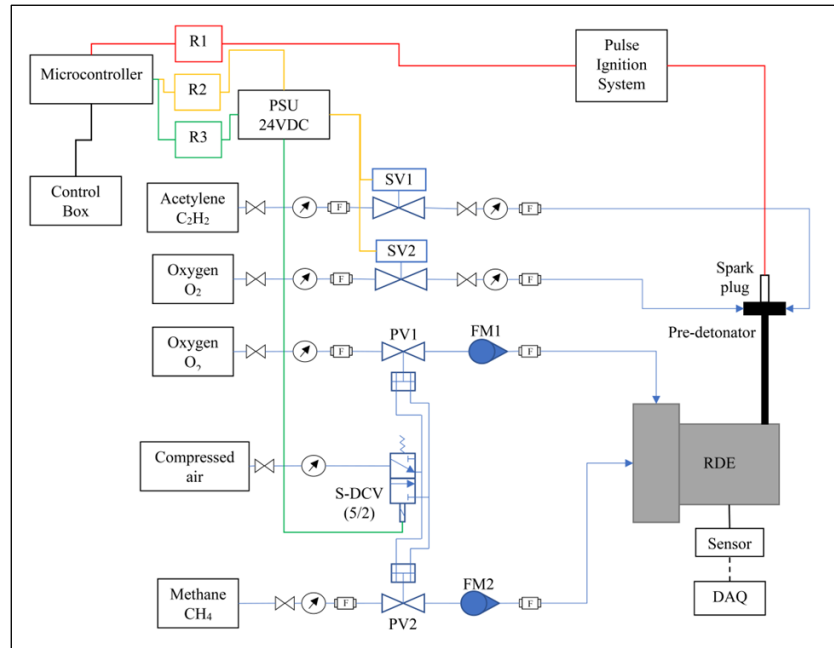


Fig. 3. RDE control system including the fuel-oxidizer feeding (blue line), ignition (red line), and operation sequence (green line).

Fig 4 presents the basic sequence for the RDE operation applied in this study. The supply valves for RDE and pre-detoner will be activated at the beginning of the experiment. After 'a' second, the pre-detoner valves closed and left the RDE combustion chamber valves to remain open. Then, the ignition initiation of the pre-detoner will be activated after 'b' second. Consequently, the detonation wave will be developed and propagate within the RDE combustion chamber. Towards the end of the RDE operation, after 'c' second, the RDE valves will be closed. Note that the value for 'a', 'b' and 'c' can be modified to the sequential control subsystem. In this study, the value for 'a', 'b' and 'c' were set to 100 ms, 100 ms, and 500 ms, respectively.

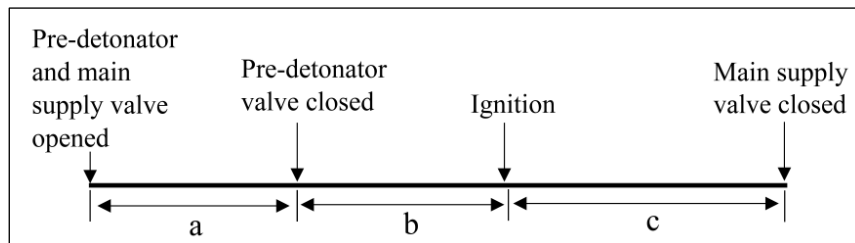


Fig. 4. RDE operation sequence.

## Measuring devices

As mentioned, a high-frequency ICP pressure sensor has been used to capture the pressure profile during the RDE operation. The high-frequency ICP pressure sensor used is PCB Piezotronics 113B24, which has a sensitivity of 5.06 mV/psi. Since no water jacket was applied to the pressure sensor, the duration of the RDE hot test in this study was limited to 500 ms or less. This approach was taken to protect the pressure sensor from getting damage as suggested by previous study (Huang et al., 2023; Wang et al., 2025; Yang et al., 2023). Furthermore, the environment during the RDE operation can be considered harsh since it is highly related to blasts and shock fronts that may cause high flash temperatures. Thus, to lower the effects on the signals captured, black vinyl electrical tape was used to insulate the pressure sensor diaphragm thermally.

On the other hand, Kistler Quartz Force Link (9331B) was attached to the tray that holds the RDE at a fixed location. The force link sensor will capture any rapid changes in the compression and tensile forces during the RDE operation. Thus, using the force link sensor in this study would be valuable in confirming the operational timeframe of the RDE operation sequence. Moreover, the digital data acquired from the high-frequency ICP pressure sensor and the force link sensor are fed to the same DAQ system, which comprises a PCI-6133 data acquisition card that is connected to the shielded connector block (BNC-2120), signal conditioner (Kistler Type 5148), and post-processing software.

## RESULTS AND DISCUSSION

This study focuses on exploring performance behaviour during the operation of the present small-scale RDE. This includes the detonation stability, which may influence the detonation wave velocity and sustainability within the RDE, as unstable detonation waves may affect the overall performance and may cause operational failure. Additionally, stable, and sustained detonation waves may result in consistent thrust generation. Thus, the performance characteristics of the small-scale RDE at different equivalence ratios ( $\varphi = 0.8$  to  $\varphi = 1.2$ ) with the total mass flow rate,  $\dot{m}_{total}$ , of 0.0040 kg/s have been investigated and discussed as follows.

Based on the experimental observations, the pressure profiles obtained for each tested equivalence ratio in this study have consistently displayed signs of instability. These instabilities were characterised mainly by two observed patterns: chaotic instability and amplitude modulation, commonly referred to as waxing and waning instability. Although the pressure profiles for each equivalence ratio tested have different instability intensities, two representative cases are represented in Fig 5 to illustrate the typical instability modes observed in this study. Fig 5(a) demonstrates a chaotic instability shown by the irregular and non-periodic oscillations of the pressure amplitude at  $\varphi = 0.8$ . Meanwhile, variation in the pressure amplitude modulation, which characterised the waxing and waning instability, is presented by Fig 5(b) for the case of  $\varphi = 0.9$ .

Furthermore, the pressure profile for each equivalence ratio tested in this study was analysed, and the summary of the results is presented in Table 2. At  $\varphi = 0.8$ , chaotic instability was observed from the pressure profile with no clear indication of waxing and waning instability. As the equivalence ratio increased to 0.9, waxing and waning instability can be slightly seen from the pressure profile, accompanied by dominant chaotic instability with lesser intensity than  $\varphi = 0.8$ . At  $\varphi = 1.0$ , the amplitude of waxing and waning instability was clear with very few indications of chaotic pressure fluctuations. When the equivalence ratio increased to 1.1, the pressure profile was slightly similar to the case  $\varphi = 1.0$ , but with a higher-pressure peak, more significant waxing and waning, and stronger indications of chaotic pressure fluctuations. The pressure profile trends for  $\varphi = 1.2$  show a combination of multiple patterns of chaotic and waxing and waning, with some regions the pressure peaks appear to be higher than  $\varphi = 1.1$ . Meanwhile, most of the

pressure profile show lower pressure peaks than  $\varphi = 1.1$ . The waxing and waning instability was clearly observed at  $\varphi = 1.2$  with significant traces of chaotic pressure behaviour across the pressure profile.

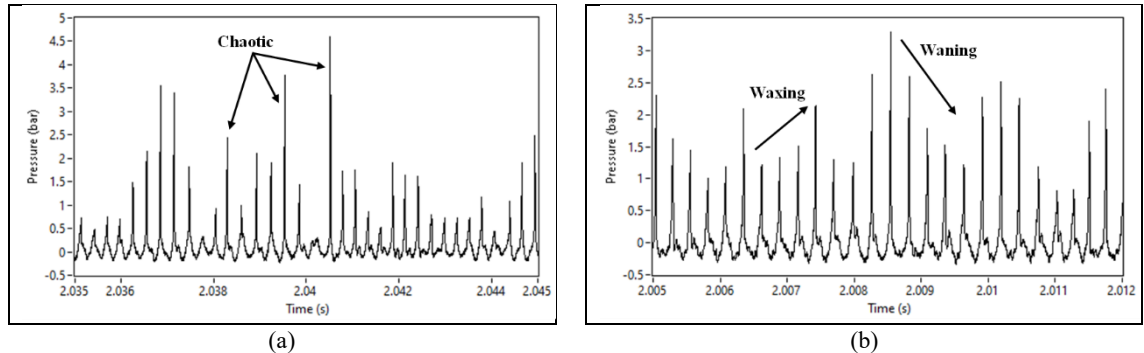


Fig. 5. Representative pressure traces showing (a) chaotic instability taken from  $\varphi = 0.8$  and (b) waxing and waning instability taken from  $\varphi = 0.9$  in the present small-scale RDE.

Table 2. Qualitative assessment of the chaotic instability and waxing and waning instability for  $\dot{m}_{total}$  of 0.0040 kg/s at different equivalence ratios

Equivalence ratio	Chaotic instability	Waxing and waning instability	Remarks
0.8	High	No clear indication	Clearly shows irregular amplitude fluctuations and a lack of periodic structure.
0.9	Moderate	Minor	Irregular amplitude fluctuations are still dominant, with minor traces of waxing and waning.
1.0	Minor	Low	Clear rise and fall of pressure amplitude with minor traces of amplitude fluctuations
1.1	Moderate	Moderate	Clear rise and fall of pressure amplitude with stronger irregular pressure amplitudes
1.2	High	High	The waxing and waning envelope can be seen and dominant, with high-pressure amplitude irregularity and spike density.

In general, chaotic instability occurs under low air injection pressure ratios, fuel-lean conditions, and large fuel injection orifice conditions (Anand et al., 2016). It was observed in this study that the intensity of the chaotic instability decreases as the equivalence ratio approaches the stoichiometric condition. This observation is supported by Li et al. (2018), which reported that the detonation wave propagation stability is influenced by the change in the equivalence ratio, with leaner reactant mixture leading to higher frequency fluctuation. Moreover, the chaotic instability became minimal at the stoichiometric condition and increased again beyond this point. This can be seen by the case  $\varphi = 0.8$  and  $\varphi = 1.2$ , representing the fuel-lean and fuel-rich mixtures, respectively, where both clearly show high chaotic instability from the pressure profile. In addition to the influence of the fuel and oxidizer composition, the presence of chaotic instability is closely related to the pressure feedback experience during the experiment. The pressure feedback affects the reactant injectors and causes improper mixing, leading to chaotic instability. Furthermore, the waxing and waning instability may also be caused by the inconsistent fuel and oxidizer supply pressure due to periodic clearance and obstruction of the reactant injectors.

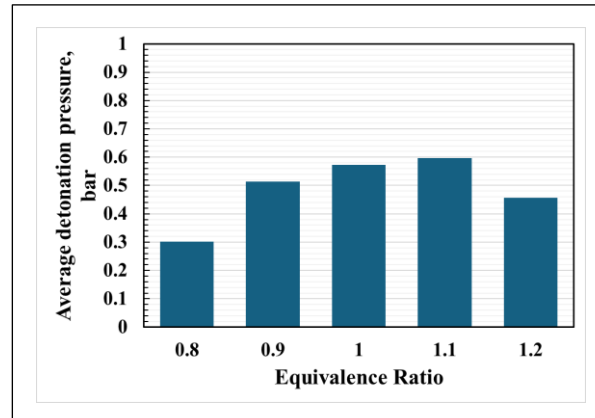


Fig. 6. Average detonation pressure within the small-scale RDE.

Additionally, the average detonation pressure within the small-scale RDE annulus has been observed to rise as the equivalence ratio increases, reaching a maximum value at  $\varphi = 1.1$  before decreasing as the equivalence ratio continues to increase, as presented in Fig 6. A similar finding has been reported by Jing & Ma (2024) where the average peak pressure first increased, reached the maximum value, and then decreased gradually. This finding shows that the detonation wave for the case with a lower equivalence ratio may have been sustained, but not to the optimal pressure levels. As the equivalence ratio increases, the pressure curves rise because of better combustion efficiency that improves the detonation characteristics. However, the detonation performance decreases and experiences instability when the equivalence ratio is further increased beyond the optimal range due to excessive fuel, which disrupts combustion efficiency. The optimal pressure range for the RDE combustion chamber is critical for achieving the desired thermodynamic efficiency and thrust performance (Xue et al., 2022).

Subsequently, Fast Fourier Transformation (FFT) has been performed on the data obtained from the high-frequency pressure sensors and generated the plot as presented in Fig 7. According to Lu et al. (2025), the frequency corresponding to the highest amplitude represents the detonation frequency of the detonation wave within the combustor during the RDE operation and is denoted as the dominant frequency. As shown in Fig 7, the dominant frequency increased with the rising equivalence ratio from  $\varphi = 0.8$  to  $\varphi = 1.2$ , indicating an intensity increment of the detonation wave. This finding is consistent with Xue et al. (2022), where the increment to the equivalence ratio may increase the detonation wave intensity and frequency while decreasing the detonation wave establishment period. In addition, the FFT trend shown in Fig 7 also indicates the presence of multiple non-dominant frequencies, which are similar to the studies reported by Li et al. (2018) and Zhou et al. (2018). The non-dominant frequencies observed in the FFT spectrum may influence the characteristics of the detonation wave propagation during the RDE operation, resulting in a complex and dynamic behaviour.

As reported by Li et al. (2018), the existence of multiple non-dominant frequencies resulted from the transient propagation behaviour, such as the dual-wave to single-wave transitions, where the significant frequency peaks were linked to the different detonation counts. Moreover, Zhou et al. (2018) have reported that multiple frequency components may be due to strong-weak detonation wave alternation and may occur during the formation process, such as in the early unstable phase. Note that the strong-weak detonation wave alternation refers to the propagation of a dual detonation wave, which consists of a strong pressure wave followed by relatively weak waves. Based on the findings observed by Li et al. (2018) and Zhou et al. (2018), the non-dominant frequencies identified in this study may occur from conditions such as multiple wave propagation modes or transient instabilities such as pressure feedback, wave emergence or incomplete detonation formation.

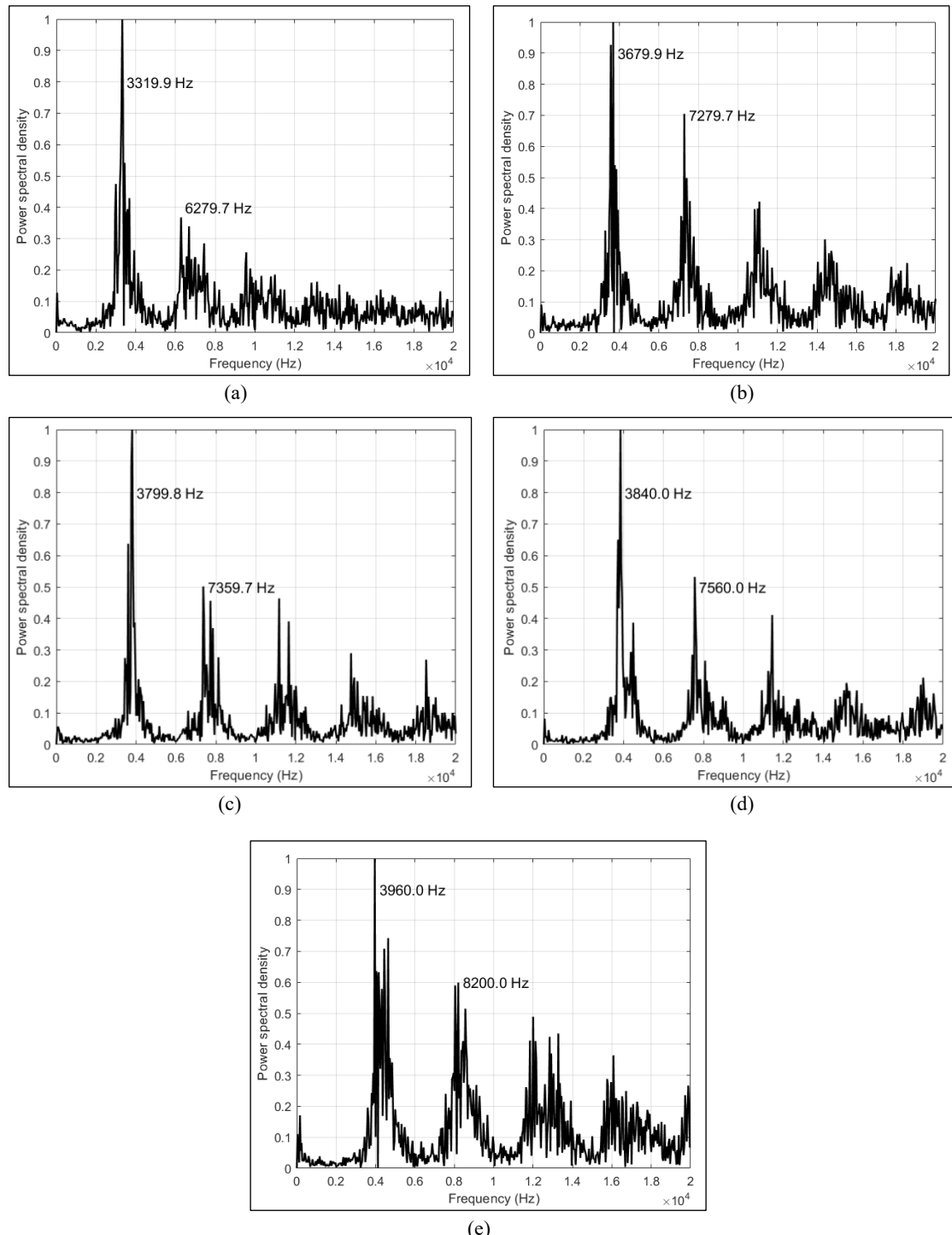


Fig. 7. FFT spectrum in the range of 0 to 20 kHz at different equivalence ratio (a)  $\varphi = 0.8$ , (b)  $\varphi = 0.9$ , (c)  $\varphi = 1.0$ , (d)  $\varphi = 1.1$ , and (e)  $\varphi = 1.2$ .

Further analysis has been conducted by determining the detonation wave velocity and thrust based on the dominant frequency obtained from the FFT spectrum, as suggested by Li et al. (2018). Fig 8 shows the average detonation velocity and thrust for each equivalence ratio obtained in this study. The average detonation velocity for each equivalence ratio obtained in this study ranges between 479 m/s and 572 m/s. The average detonation velocity was found to increase with the equivalence ratio increment. However, the increment in average detonation velocity from  $\varphi = 0.9$  to  $\varphi = 1.2$  was observed to be gradual, with 1% – 3.3% difference between each equivalence ratio. On the other hand, the difference in the average detonation velocity between  $\varphi = 0.8$  and  $\varphi = 0.9$  showed more significant differences, with the variation of approximately 10.8%.

A study conducted by Mazlan et al. (2023) has reported on the detonation wave velocity for the methane-oxygen reactants based on the ideal Chapman-Jouguet (CJ) estimation for the equivalence ratio range from 0.5 to 3.0. The results showed that the detonation wave velocity increased initially, but the increment rate was slowly reduced, reaching the peak detonation wave velocity observed at  $\varphi = 1.9$ . Beyond this point, the detonation wave velocity decreased with further increments in the equivalence ratio. It is important to highlight that the equivalence ratio range tested in the present study was limited to  $\varphi = 1.2$ . Therefore, it is possible that this study did not fully capture the maximum detonation wave velocity for methane-oxygen reactants as predicted by CJ estimation. Nevertheless, the characteristics of an approaching peak detonation wave velocity were observed in this study, as the gradual increment in the detonation wave velocity was observed when the equivalence ratio increased from 0.9 to 1.2.

These average detonation velocity values were then compared with the ideal CJ estimation values for methane-oxygen mixtures as reported by Mazlan et al. (2023). It was found that the average detonation velocities derived from the FFT analysis in this study correspond to only 20% – 23% of the estimated ideal CJ values. Although the average detonation velocities obtained in this study are significantly lower than the estimated ideal CJ values, the dominant operating frequencies recorded during the RDE operation are higher than the typically observed frequencies in PDE and fall within the RDE operating frequency range as reported by Liu et al. (2023). Based on these findings, the RDE operation in this study can be considered successful as shown by the operating frequency characteristics despite the average detonation velocity deficit compared to the ideal CJ values. This highlights the potential of the current RDE configuration, with the need for further optimization to improve the detonation propagation during the RDE operation.

From the average detonation velocities obtained, the thrust generated during the RDE operation was calculated and presented in Fig 8. It was found that the trend for the thrust generated closely followed the trend of the average detonation velocity. The resulting thrust values were increased as the equivalence ratio increased from 0.8 to 1.2, with a range of 1.9 N to 2.3 N. It is noted that the thrust obtained in this study is relatively low. This situation is influenced by the low total mass flow rate implemented during the current RDE operation and agrees with the findings reported by Law et al. (2021). Additionally, other factors may also contribute to this condition, such as the tendency of the detonation wave to propagate upstream, which can generate pressure feedback to the reactant inlet, cause disruptions during the reactant mixing process, and affect the thrust generation (Wang et al., 2021). On the other hand, the attachment of the nozzle at the RDE exhaust has been reported to enhance the thrust output by increasing the exhaust velocity during the RDE operation (Han et al., 2021; Law et al., 2021; Xie et al., 2020). Furthermore, constricting the annulus channel before the nozzle may increase the local static pressure and enhance the detonation process in the RDE combustion chamber (Fotia et al., 2016).

Accordingly, the detonation wave stability results, average detonation wave velocity, and thrust have been reported. These three key areas are interdependent and play a critical role in evaluating the RDE performance. Based on the results presented, variation in the equivalence ratio influences the combustion dynamics and detonation wave propagation characteristics, affecting the stability and performance of the small-scale RDE. This is supported by Bennewitz et al. (2023), which stated that the equivalence ratio controls the reactants' chemistry and influences the detonation characteristics.

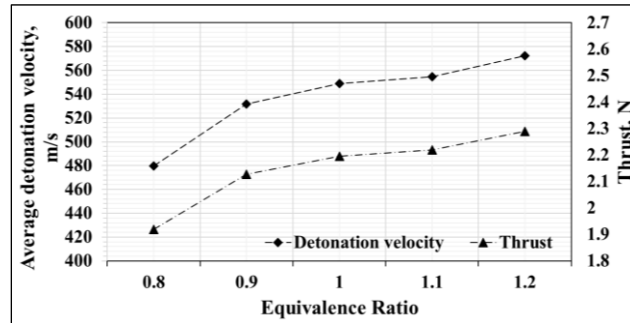


Fig. 8. Average detonation velocity and thrust.

Thus, it is important to identify the critical equivalence ratio that optimises the detonation wave stability and maintains a proper balance between the reactants to avoid insufficient or excessive fuel conditions that could affect the overall performance, especially for small-scale RDE with a small channel radius (Kudo et al., 2011; Mundt et al., 2024). Note that the geometrical parameters influence the operational stability of the RDE and define the operational limits for the fuel and oxidizer (Mundt et al., 2024). Among the tested operating conditions in this study, the least occurrence of instabilities was found at  $\varphi = 1.0$ , which indicates a good balance between the fuel-oxidizer mixture and the detonation wave stability.

Furthermore, both average detonation velocity and thrust increased as the equivalence ratio increased from 0.8 to 1.2, gradually increasing beyond the  $\varphi = 0.9$ . Interestingly, the highest thrust estimated based on the average detonation velocity in this study was recorded at  $\varphi = 1.2$ , while the average chamber pressure peaked slightly earlier at  $\varphi = 1.1$ . Although the highest thrust was determined at  $\varphi = 1.2$ , it is important to note that this value was estimated based on the average detonation velocity, referring to the FFT output. Since the pressure profile at  $\varphi = 1.2$  indicated significant instabilities during the RDE operation, the calculated average may not fully capture the transient losses or variation, as the actual thrust performance may have fluctuated considerably. Thus, the actual thrust at  $\varphi = 1.2$  could be potentially lower than the value estimated in this study.

As previously stated, only chaotic instability and waxing and waning instability were identified from the pressure profile obtained in this study. It is noted that LPD instability can only be detected with more than one pressure sensor placed axially along the combustor. However, this study used only a single pressure sensor to obtain the pressure profile. Furthermore, mode switching instability is associated with the operating mode changes and is closely related to the number of detonation waves during the experiment. This phenomenon can be visualized using high-speed imaging techniques. However, this technique could not be implemented in this study due to image interference caused by the insulation applied to the pressure sensor during the RDE operation. Although there were limitations in verifying all four types of instabilities, the results obtained are considered sufficient to assess the operational capability of the RDE.

## CONCLUSION

This study presented a small-scale RDE operation's performance characteristic by analysing the detonation wave stability, average detonation velocity, thrust, and average chamber pressure across a range of equivalence ratios. The results demonstrated that these performance criteria are interdependent and influence engine behaviour. Some of the remarkable conclusions made from this study are as follows:

- Chaotic instability and waxing and waning instability were observed from the pressure profiles obtained. The least instability occurrence was observed at  $\varphi = 1.0$ , which can be considered the optimal mixture proportion for a stable RDE operation.
- These instabilities might be due to improper mixing caused by pressure feedback and periodic obstruction and clearance of the reactant injectors.
- The average detonation velocity and thrust were found to increase as the equivalence ratio increases from 0.8 to 1.2. Gradual average detonation velocity increments were observed as the equivalence ratio rose beyond  $\varphi = 0.9$ , indicating that further equivalence ratio increments towards richer mixtures resulted in only minor improvement in the average detonation velocity and thrust generated.
- The average detonation pressure within the RDE annulus has risen, reaching a maximum value, and decreasing as the equivalence ratio increases. This indicates an optimal condition that results in the maximum average detonation pressure.
- A well-balanced reactant mixture is important to ensure stable RDE operation and maximise the performance of the RDE.

Although the data obtained on the performance characteristics during the small-scale RDE operation in this study have certain limitations, they still provide a foundation for enhancing future small-scale RDE operations. Further investigations are required to ensure an optimized small-scale RDE performance and to produce consistent thrust. For future work, it is recommended that a number of high-frequency pressure diagnostics and time-resolved thrust measurements be implemented to capture the transient behavior of RDE operation better. In addition, incorporating optical diagnostics such as Schlieren or chemiluminescence imaging techniques could help to visualize the wave propagation and identify the instability modes. A parametric study of the type of fuels, RDE geometries, or injection strategies would further contribute to understanding and optimizing RDE performance.

## ACKNOWLEDGEMENT

The research was supported by Universiti Teknologi Malaysia through the High Impact Research Grant with cost centre number Q.J130000.2451.09G05.

## CONFLICT OF INTEREST STATEMENT

The authors agree that this research was conducted in the absence of any self-benefits, commercial or financial conflicts and declare the absence of conflicting interests with the funders.

## AUTHOR'S CONTRIBUTION

The authors confirm their contribution to the paper as follows: study conception and design: Mohd Fahmi Md Salleh, Mazlan Abdul Wahid, Natrah Kamaruzaman; data collection: Mohd Fahmi Md Salleh; analysis and interpretation of results: Mohd Fahmi Md Salleh, Mazlan Abdul Wahid, Umar Ikhwan Mohd Rozaiddin; draft manuscript preparation: Mohd Fahmi Md Salleh, Hazim Sharudin, Haszeme Abu Kasim, Ab Aziz Mohd Yusof. All authors reviewed the results and approved the final version of the manuscript.

## REFERENCE

Anand, V., George, A. S., Driscoll, R., & Gutmark, E. (2016). Analysis of air inlet and fuel plenum behavior in a rotating detonation combustor. *Experimental Thermal and Fluid Science*, 70, 408–416.

Anand, V., George, A. S., Driscoll, R., & Gutmark, E. (2015). Characterization of instabilities in a rotating detonation combustor. *International Journal of Hydrogen Energy*, 40(46), 16649–16659.

Armbruster, W., Börner, M., Bee, A., Martin, J., Knapp, B., General, S., Hardi, J., & Bard, E. (2024). Experimental investigation of a small-scale oxygen-hydrogen rotating detonation rocket combustor. *AIAA SciTech Forum and Exposition* (pp. 1-10). American Institute of Aeronautics and Astronautics.

Barnouin, P., Paschereit, C. O., Bach, E., & Bohon, M. D. (2025). Dynamics and interactions of counter-rotating waves in rotating detonation combustors. *Experimental Thermal and Fluid Science*, 168, 111486.

Bennewitz, J. W., Burr, J. R., Bigler, B. R., Burke, R. F., Lemcherfi, A., Mundt, T., Rezzag, T., Plaehn, E. W., Sosa, J., Walters, I. V., Schumaker, S. A., Ahmed, K. A., Slabaugh, C. D., Knowlen, C., & Hargus Jr, W. A. (2023). Experimental validation of rotating detonation for rocket propulsion. *Scientific Reports*, 13, 14204.

Bykovskii, F. A., & Vedernikov, E. F. (2003). Continuous detonation of a subsonic flow of a propellant. *Combustion, Explosion and Shock Waves*, 39(3), 323-334.

Bykovskii, F. A., Zhdan, S. A., & Vedernikov, E. F. (2006). Continuous spin detonations. *Journal of Propulsion and Power*, 22(6), 1204–1216.

Bykovskii, F. A., Zhdan, S. A., & Vedernikov, E. F. (2018). Continuous detonation of methane/hydrogen–air mixtures in an annular cylindrical combustor. *Combustion, Explosion and Shock Waves*, 54(4), 472–481.

Dairobi G, A., Wahid, M. A., Mazlan, M. A., & Azeman, M. H. (2021). Early assessment of asymmetric vortex small rotating detonation engine. *Evergreen*, 8(1), 182–186.

Dechert, J. R., Polanka, M. D., Schauer, F. R., Schumaker, S. A., Sell, B., & Fotia, M. L. (2020). Development of a small scale rotating detonation engine. *AIAA Scitech 2020 Forum* (pp. 1–11). American Institute of Aeronautics and Astronautics.

Driscoll, R. B. (2016). Investigation of sustained detonation devices: the pulse detonation engine-crossover system and the rotating detonation engine system [Doctoral thesis, University of Cincinnati].

Driscoll, R., Anand, V., St. George, A., & Gutmark, E. (2015). Investigation on RDE operation by geometric variation of the combustor annulus and nozzle exit area. *9th U.S. National Combustion Meeting* (pp. 1-10). Central States Section of the Combustion Institute.

Fotia, M. L., Schauer, F., Kaemming, T., & Hoke, J. (2016). Experimental study of the performance of a rotating detonation engine with nozzle. *Journal of Propulsion and Power*, 32(3), 674–681.

Frolov, S. M., Aksenov, V. S., Ivanov, V. S., & Shamshin, I. O. (2015). Large-scale hydrogen-air continuous detonation combustor. *International Journal of Hydrogen Energy*, 40(3), 1616-1623.

Goodwin, G. B., Houim, R. W., & Oran, E. S. (2016). Effect of decreasing blockage ratio on DDT in small channels with obstacles. *Combustion and Flame*, 173, 16–26.

Han, H. S., Lee, E. S., & Choi, J. Y. (2021). Experimental investigation of detonation propagation modes

and thrust performance in a small rotating detonation engine using C<sub>2</sub>H<sub>4</sub>/O<sub>2</sub> propellant. *Energies*, 14(5), 1381.

Heiser, W. H., & Pratt, D. T. (2002). Thermodynamic cycle analysis of pulse detonation engines. *Journal of Propulsion and Power*, 18(1), 68–76.

Hoke, J. L., Bradley, R. P., & Schauer, F. R. (2005). Impact of DDT mechanism, combustion wave speed, temperature, and charge quality on pulsed-detonation-engine performance. 43rd AIAA Aerospace Sciences Meeting and Exhibit (pp. 1-9). American Institute of Aeronautics and Astronautics.

Hu, J., & Zhang, B. (2024). Time/ frequency domain analysis of detonation wave propagation mechanism in a linear rotating detonation combustor. *Applied Thermal Engineering*, 255, 124014.

Huang, S. Y., Zhou, J., Liu, W. D., Liu, S. J., Peng, H. Y., Zhang, H. L., & Yuan, X. Q. (2023). Analysis on the radial structure of rotating detonation wave in a hollow combustor. *Fuel*, 348, 128581.

Jing, J., & Ma, H. (2024). An experimental study on gas-solid two-phase rotating detonation ramjet engine based on aluminum powder fuel. *Journal of Physics: Conference Series*, 2764(1), 12032.

Kindracki, J. (2015). Experimental research on rotating detonation in liquid fuel-gaseous air mixtures. *Aerospace Science and Technology*, 43, 445–453.

Kindracki, J., Wolański, P., & Gut, Z. (2011). Experimental research on the rotating detonation in gaseous fuels-oxygen mixtures. *Shock Waves*, 21(2), 75–84.

Kudo, Y., Nagura, Y., Kasahara, J., Sasamoto, Y., & Matsuo, A. (2011). Oblique detonation waves stabilized in rectangular-cross-section bent tubes. *Proceedings of the Combustion Institute*, 33(2), 2319–2326.

Law, H., Baxter, T., Ryan, C., & Deiterding, R. (2021). Design and testing of a small-scale laboratory rotating detonation engine running on ethylene-oxygen. *AIAA Propulsion and Energy Forum* (pp. 1–15). American Institute of Aeronautics and Astronautics.

Li, B., Wu, Y., Weng, C., Zheng, Q., & Wei, W. (2018). Influence of equivalence ratio on the propagation characteristics of rotating detonation wave. *Experimental Thermal and Fluid Science*, 93, 366–378.

Lin, W., Zhou, J., Liu, S., Lin, Z., & Zhuang, F. (2015). Experimental study on propagation mode of H<sub>2</sub>/air continuously rotating detonation wave. *International Journal of Hydrogen Energy*, 40(4), 1980–1993.

Liu, H., Song, F., Jin, D., Xu, S., & Yang, X. (2023). Experimental investigation on spray and detonation initiation characteristics of premixed/ non-premixed RDE. *Fuel*, 331(2), 125949.

Lu, S., Zhu, Q., Gong, J., Chen, H., & Ying, H. (2025). Experimental study on transpiration cooling with phase change in rotating detonation engine. *Applied Thermal Engineering*, 258(A), 124633.

Mazlan, M. A., Yasin, M. F. M., Saat, A., Wahid, M. A., Ghazali, A. D., & Azeman, H. (2023). Wave propagation characteristics in predetonator of rotating detonation engine. *AIP Conference Proceedings*, 2749, 70009.

Mazlan, M. A., Yasin, M. F. M., Saat, A., Wahid, M. A., Ghazali, A. D., & Rahman, M. N. (2021). Initiation characteristics of rotating supersonic combustion engine. *Evergreen*, 8(1), 177–181.

Mundt, T., Knowlen, C., & Kurosaka, M. (2024). Scale effects on rotating detonation rocket engine operation. *Applications in Energy and Combustion Science*, 19, 100282.

Paxson, D. E., Fotia, M. L., Hoke, J., & Schauer, F. (2015). Comparison of numerically simulated and <https://doi.org/10.24191/jmeche.v23i1.6123>

experimentally measured performance of a rotating detonation engine. 53rd AIAA Aerospace Sciences Meeting (pp. 1-11). American Institute of Aeronautics and Astronautics.

Prakash, S., Raman, V., Lietz, C. F., Hargus, W. A., & Schumaker, S. A. (2021). Numerical simulation of a methane-oxygen rotating detonation rocket engine. *Proceedings of the Combustion Institute*, 38(3), 3777–3786.

Rahman, M. N. (2021). Numerical analysis of detonation stability in a rotating detonation engine fueled with biogas and hydrogen [Doctoral thesis, Universiti Teknologi Malaysia]. Retrieved from <http://eprints.utm.my/102567/>

Rahman, M. N., Wahid, M. A., & Mohd Yasin, M. F. (2020). Predictive numerical analysis on the fuel homogeneity in a rotating detonation engine (RDE) implementing radially-entered fuel injection scheme. *IOP Conference Series: Materials Science and Engineering*, 884, 012109.

Raman, V., Prakash, S., & Gamba, M. (2023). Nonidealities in rotating detonation engines. *Annual Review of Fluid Mechanics*, 55, 639-674.

Rankin, B. A., Richardson, D. R., Caswell, A. W., Naples, A., Hoke, J. L., & Schauer, F. R. (2015). Imaging of OH\* chemiluminescence in an optically accessible nonpremixed rotating detonation engine. 53rd AIAA Aerospace Sciences Meeting (pp. 1-16). American Institute of Aeronautics and Astronautics.

Rui, Z., Dan, W., & Jianping, W. (2016). Progress of continuously rotating detonation engines. *Chinese Journal of Aeronautics*, 29(1), 15–29.

Wang, J., Han, J., Bai, Q., Liu, Z., Zheng, Q., & Weng, C. (2025). Experimental study on rotating detonation characteristics and multiple waves evolution mechanisms in CH<sub>4</sub>/CO/H<sub>2</sub> gas mixtures. *International Journal of Hydrogen Energy*, 115, 101–112.

Wang, Y., Qiao, W., & Jialingle (2021). Combustion characteristics in rotating detonation engines. *International Journal of Aerospace Engineering*, 2021(1), 8839967.

Xie, Q., Ji, Z., Wen, H., Ren, Z., Wolanski, P., & Wang, B. (2020). Review on the rotating detonation engine and its typical problems. *Transactions on Aerospace Research*, 2020(4), 107–163.

Xue, S., Ying, Z., Ma, H., & Zhou, C. (2022). Experimental investigation on two-phase rotating detonation fueled by kerosene in a hollow directed combustor. *Frontiers in Energy Research*, 10, 951177.

Yang, X., Song, F., Wu, Y., Zhou, J., Chen, X., Kang, J., & Ma, Y. (2023). Experimental study on suppressing pressure feedback and combustion product backflow of the rotating detonation engine. *Aerospace Science and Technology*, 141, 108523.

Zhou, S., Ma, H., Ma, Y., Zhou, C., Liu, D., & Li, S. (2018). Experimental study on a rotating detonation combustor with an axial-flow turbine. *Acta Astronautica*, 151, 7–14.

Zhu, Y. F., Xu, G. Y., Wang, C. G., Gong, L. K., & Wang, J. N. (2020). Study on acoustic detection of the working state of pulse detonation engine. *International Journal of Turbo and Jet Engines*, 37(1), 71.